Effect of Viscous Dissipation on Fully Developed Laminar Heat Transfer of Power-Law Non-Newtonian Fluids in Plane Couette-Poiseuille Flow

by

Ganbat DAVAA*, Toru SHIGECHI**
and Satoru MOMOKI**

Fully developed laminar heat transfer of a non-Newtonian fluid flowing between two parallel plates with one moving plate was analyzed taking into account the viscous dissipation of the flowing fluid. Applying the velocity profile obtained for the plane Couette-Poiseuille laminar flow, the energy equation with the viscous dissipation term was exactly solved for the boundary conditions of constant wall heat flux at one wall with the other insulated. The effects of the relative velocity of a moving plate, flow index and Brinkman number on Nusselt numbers at the plate walls were discussed.

1. Introduction

Problems involving fluid flow and heat transfer with an axially moving core of solid body or fluid in an annular geometry can be found in many manufacturing processes, such as extrusion, drawing and hot rolling, etc. In such processes, a hot plate or cylindrical rod continuously exchanges heat with the surrounding environment. For such cases, the fluid involved may be Newtonian or non-Newtonian and the flow situations encountered can be either laminar or turbulent.

In the previous study[1], fully developed laminar heat transfer of a Newtonian fluid flowing between two parallel plates with one moving plate was analyzed taking into account the viscous dissipation of the flowing fluid.

In the previous report[2], an exact solution of the momentum equation was obtained for fully developed laminar flow of a non-Newtonian fluid flowing between two parallel plates with one moving plate. The constitutive equation (i.e., the shear stress-shear rate relation) for a non-Newtonian fluid is described by the power-law model most frequently used in non-Newtonian fluid flow and heat transfer.

In this report, fully developed laminar heat transfer of a non-Newtonian fluid flowing between two parallel plates with one moving plate was analyzed taking into account the viscous dissipation of the flowing fluid. Applying the velocity distribution obtained for the plane Couette-Poiseuille laminar flow, the energy equation with the viscous dissipation term was exactly solved for the boundary conditions of constant wall heat flux at one wall with the other insulated. The effects of the relative velocity of a moving plate, flow index and Brinkman number on Nusselt numbers at the plate walls were discussed.

Nomenclature

Br	Brinkman number
c_P	specific heat at constant pressure
F	parameter
f	friction factor
k	thermal conductivity
L^*_{max}	dimensionless location at the maximum velocity (see the previous report[2])
m	consistency index
n	flow index
Nu	Nusselt number
P	pressure
q	wall heat flux
Re^*	Generalized Reynolds number

Received on April 21, 2000

* Graduate Student, School of Science and Technology

** Department of Mechanical Systems Engineering

T	temperature
u	axial velocity of fluid
u_m	average velocity of fluid
u^*	dimensionless velocity $\equiv u/u_m$
U	axial velocity of the moving plate
U^*	relative velocity of the moving plate
y	coordinate normal to the fixed plate
y^*	dimensionless coordinate $\equiv y/L$
z	axial coordinate

Greek Symbols

ρ	density
τ	shear stress
θ	dimensionless temperature

Subscripts

B	bulk
j	j = L for Case A, j = 0 for Case B
L	moving plate
0	fixed plate

2. Analysis

The physical model for the analysis is shown in Fig. 1. The lower plate is axially moving at a constant velocity. The assumptions used in the analysis are :

1. The flow is incompressible, steady-laminar, and fully developed, hydrodynamically and thermally.
2. The fluid is non-Newtonian and the shear stress may be described by the power-law model, and physical properties are constant.
3. The body forces and axial heat conduction are neglected.

2.1 Fluid Flow

The governing momentum equation together with the assumptions described above is

$$\frac{d\tau}{dy} = -\frac{dP}{dz} \tag{1}$$

The boundary conditions are :

$$\begin{cases} u = 0 \text{ at } y = 0 \\ u = U \text{ at } y = L \end{cases} \tag{2}$$

The shear stress on the left hand side of Eq. (1), τ, is given by the power-law model.

$$\tau = -m\left|\frac{du}{dy}\right|^{n-1}\frac{du}{dy} \tag{3}$$

The friction factor, f, and generalized Reynolds number, Re^*, are defined as

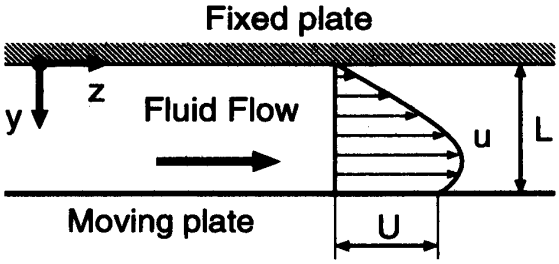

Fig. 1 Schematic of parallel plates with one moving plate

$$f \equiv \frac{L}{\rho u_m^2}\left(-\frac{dP}{dz}\right) \tag{4}$$

$$Re^* \equiv \frac{\rho u_m^{2-n}(2L)^n}{m} \tag{5}$$

The average fluid velocity, u_m, is defined as

$$u_m \equiv \frac{1}{L}\int_0^L u\,dy \tag{6}$$

Three kinds of velocity profiles across the parallel plates' passage may be assumed. The three cases are, respectively, referred to as Case Ⅰ, Case Ⅱ and Case Ⅲ.

- Case Ⅰ : The fluid maximum velocity exists between the parallel plates.
- Case Ⅱ : The fluid maximum velocity exists always on the moving plate.
- Case Ⅲ : Velocity profiles with concave shapes.

The Case Ⅰ occurs practically. Hereafter the velocity pro-

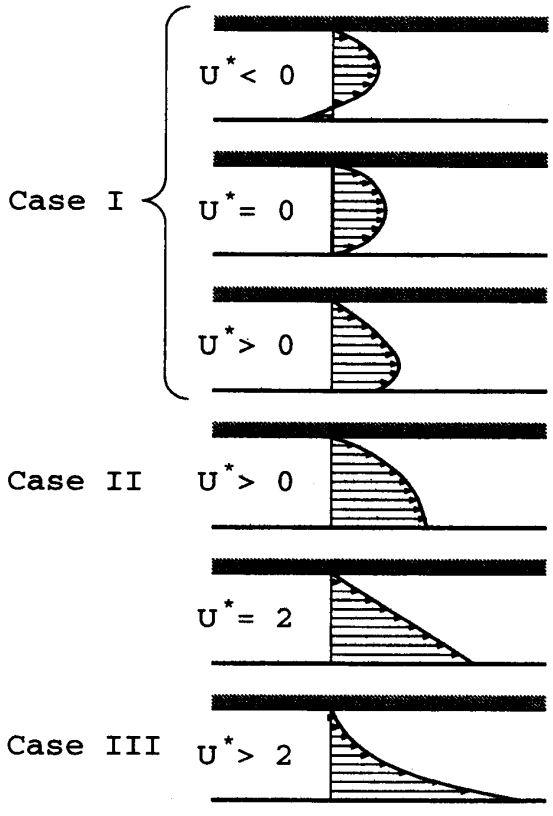

files for Case I will be examined. The velocity distributions for Case I were given in the previous report[2].

2.2 Heat Transfer

The energy equation is written as

$$k\frac{d^2T}{dy^2}-\tau\left(\frac{du}{dy}\right)=\rho c_p u\frac{dT_B}{dz} \tag{7}$$

The following two types of the thermal boundary conditions are specified :

Case A (constant heat flux at the moving plate with the fixed plate insulated) :

$$\begin{cases} -k\dfrac{\partial T}{\partial y} = 0 \text{ at } y = 0 \\ k\dfrac{\partial T}{\partial y} = q_L \text{ at } y = L \end{cases} \tag{8}$$

Case B (constant heat flux at the fixed plate with the moving plate insulated) :

$$\begin{cases} -k\dfrac{\partial T}{\partial y} = q_0 \text{ at } y = 0 \\ k\dfrac{\partial T}{\partial y} = 0 \text{ at } y = L \end{cases} \tag{9}$$

where the wall heat fluxes, q_L and q_0, are taken as positive into the fluid.

T_B is the bulk temperature defined as

$$T_B \equiv \frac{\iint_A uTdA}{\iint_A udA} \tag{10}$$

dT_B/dz is evaluated, from an energy balance, for the parallel plates, as

$$\frac{dT_B}{dz}=\frac{q_j}{\rho c_p u_m L}\left[1-\frac{\int_0^L \tau\left(\frac{du}{dy}\right)dy}{q_j}\right] \tag{11}$$

Introducing the dimensionless temperature, θ, defined as

$$\theta \equiv T/[q_j L/k] \tag{12}$$

The energy equation and the boundary conditions may be expressed in dimensionless form as

$$\frac{d^2\theta}{dy^{*2}}=u^*+Br_j\left[\left\{\int_0^1\left|\frac{du^*}{dy^*}\right|^{n+1}dy^*\right\}u^*-\left|\frac{du^*}{dy^*}\right|^{n+1}\right] \tag{13}$$

Case A :

$$\begin{cases} \dfrac{d\theta}{dy^*} = 0 \text{ at } y^* = 0 \\ \dfrac{d\theta}{dy^*} = 1 \text{ at } y^* = 1 \end{cases} \tag{14}$$

Case B :

$$\begin{cases} \dfrac{d\theta}{dy^*} = -1 \text{ at } y^* = 0 \\ \dfrac{d\theta}{dy^*} = 0 \text{ at } y^* = 1 \end{cases} \tag{15}$$

Br_j is Brinkman number, defined as

$$Br_j \equiv \left[\frac{mu_m^{n+1}}{L^n q_j}\right] \tag{16}$$

Where j = A for Case A and j = B for Case B.

The Nusselt number, Nu_j, is defined as

$$Nu_j \equiv \frac{[q_j/(T_j-T_B)]2L}{k}=\frac{2}{\theta_j-\theta_B} \tag{17}$$

where the dimensionless bulk temperature, θ_B, is defined as

$$\theta_B \equiv T_B/[q_j L/k] \tag{18}$$

$(\theta_j-\theta_B)$ is calculated as

$$\theta_j-\theta_B=\int_0^1 u^*(\theta_j-\theta)dy^* \tag{19}$$

Solving Eq. (13) together with Eq. (14) or Eq. (15), $\theta_j-\theta_B$ is obtained. The details of the results are given in Appendix.

3. Results and Discussion

Representative dimensionless temperature profiles between the parallel plates are shown in Figs. 2 and 3 for Cases A and B, regarding to the effects of viscous dissipation ($0 \le Br \le 1.0$) and relative velocity $U^* = -1.0, 0.0, 1.0$ for $n = 0.5$.

In Figs. 4 and 5, dimensionless temperature difference between wall and bulk are shown respectively for Cases A and B, regarding to the Brinkman numbers, the flow index ($n = 0.1 \sim 1.5$) and relative velocity $U^* = -1.0, 0.0, 1.0$. The temperature difference, $\theta_L-\theta_B$, decreases with increasing relative velocity, U^*, for Case A. For Case B the temperature difference, $\theta_0-\theta_B$, increases with increasing relative velocity, U^*.

In Figs. 6 and 7, Nusselt numbers are shown respectively for Case A and Case B. It is seen from these figures that Nusselt numbers, Nu_L, change sharply depending on the values of Brinkman number, Br_A, and the relative velocity of the moving plate, U^*, for Case A. Whereas for Case B Nusselt number, Nu_0, decreases gradually with an increasing Brinkman number, Br_B. The effect of viscous dissipation on Nusselt number appears more strongly in Case A than in Case B. This is due to that for Case A, the viscous dissipation effect becomes strong near the moving plate owing to the velocity profile deformed by the moving plate. Nusselt number, Nu_L, increases with increasing relative velocity U^* for Case A. However, for Case B, Nusselt number, Nu_0, decreases with increasing relative velocity U^*. Incidentally, such behavior of Nusselt numbers, Nu_L or Nu_0, is predicted by the temperature differences, $\theta_j-\theta_B$, which is inversely proportional to the Nusselt number, as defined by Eq.(A-1) and Eq.(A-8). The effect of flow index, n, on Nusselt number is seen more strongly for Case A than Case B.

4. Conclusions

The plane Couette-Poiseuille flow of power-law non-Newtonian fluid was analyzed. The present study showed that :

1. The dimensionless temperature difference, $\theta_L - \theta_B$, (Case A) decreases with increasing values of n for the case of $U^* > 0$, whereas $\theta_0 - \theta_B$, (Case B) increases with increasing values of n.
2. Nu_L (Case A) increases with increasing values of Br and n for $U^* > 0$ whereas Nu_0 (Case B) decreases with increasing values of Br and n.

References

1. T. Shigechi, et al., "Effect of viscous dissipation on fully developed heat transfer of plane Couette-Poiseuille laminar flow" *Reports of the Faculty of Engineering, Nagasaki University, vol*. 29, No. 53, 153-156 (1999).
2. Ganbat Davaa, et al., "Plane Couette-Poiseuille flow of power-law non-Newtonian fluids" *Reports of the Faculty of Engineering, Nagasaki University, vol*. 30, No. 54, 29-36 (2000).

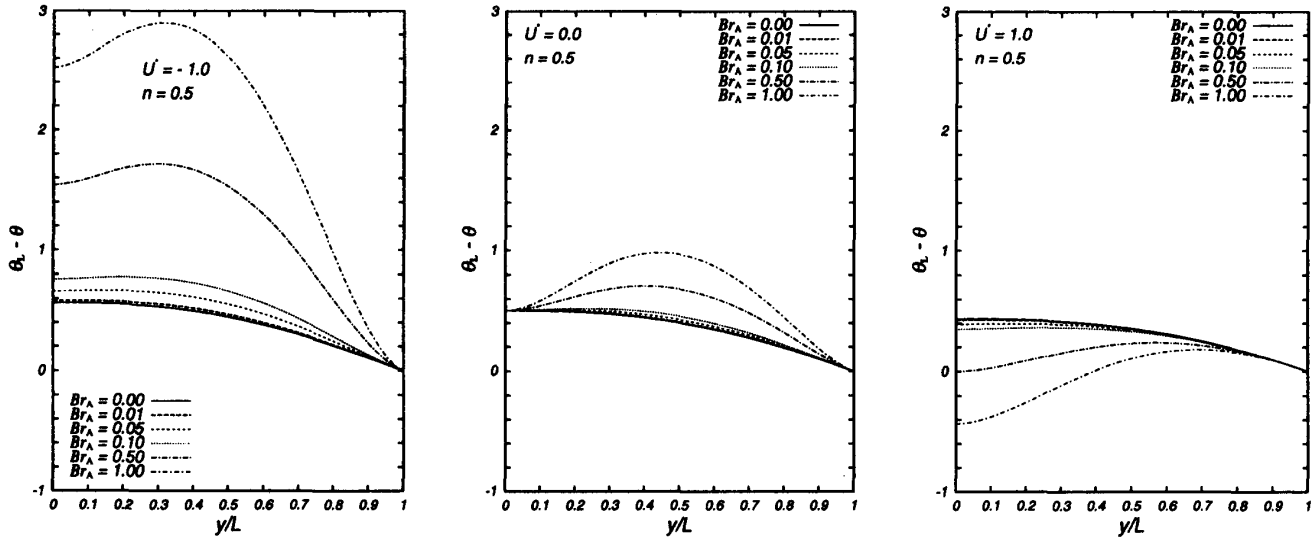

Fig. 2 Dimensionless temperature profiles for Case A

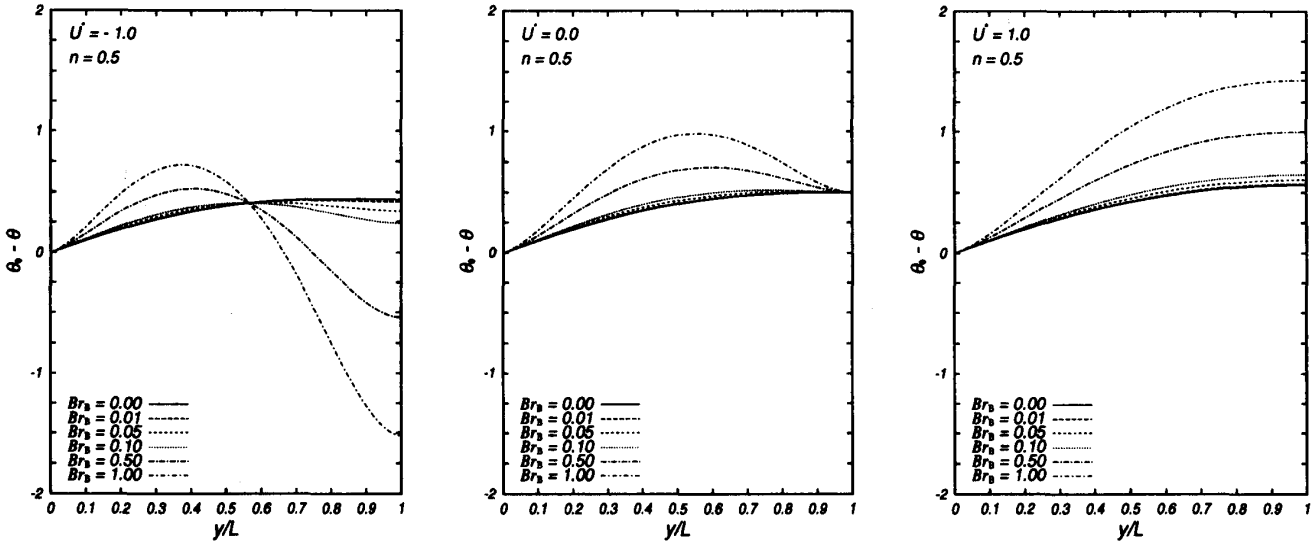

Fig. 3 Dimensionless temperature profiles for Case B

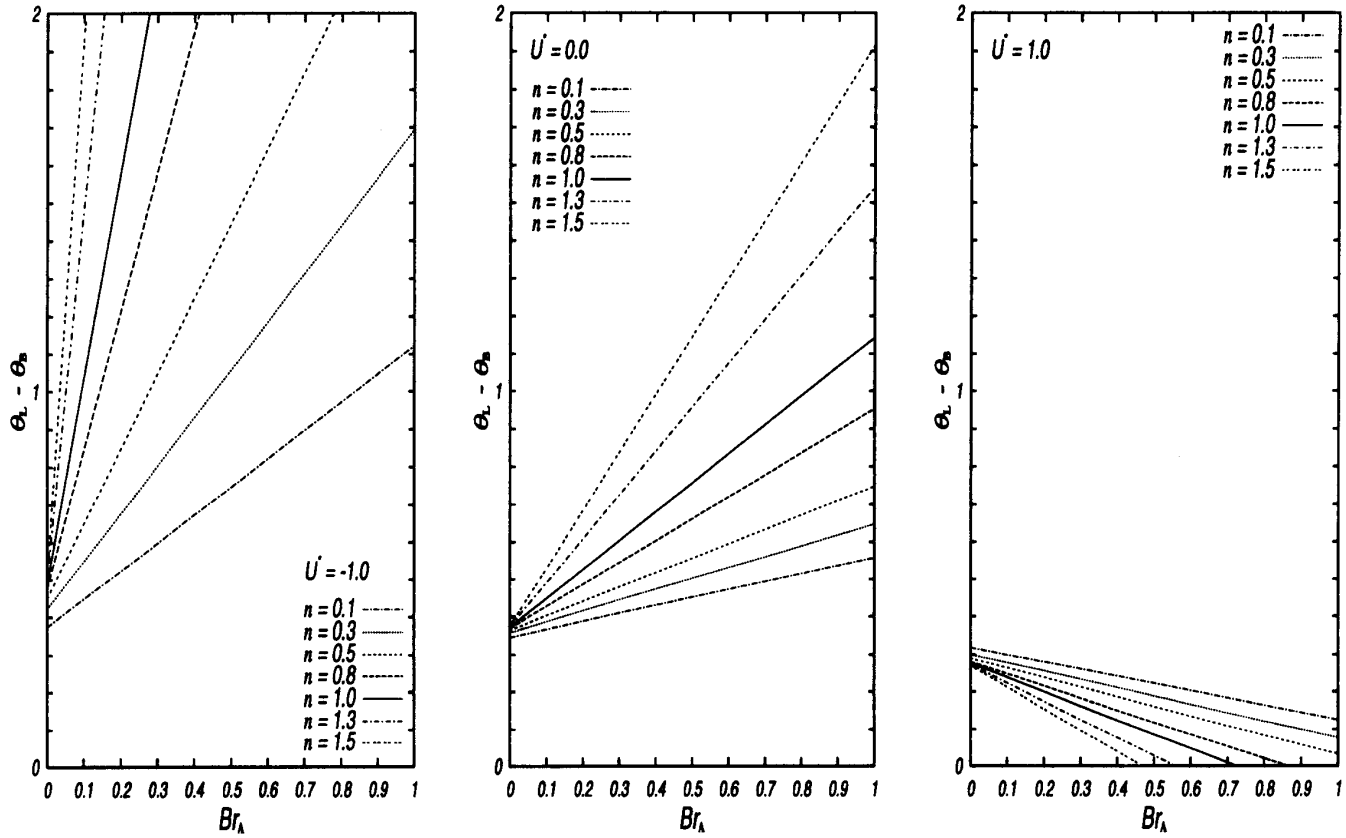

Fig. 4 Dimensionless temperature difference $(\theta_L - \theta_B)$ for Case A

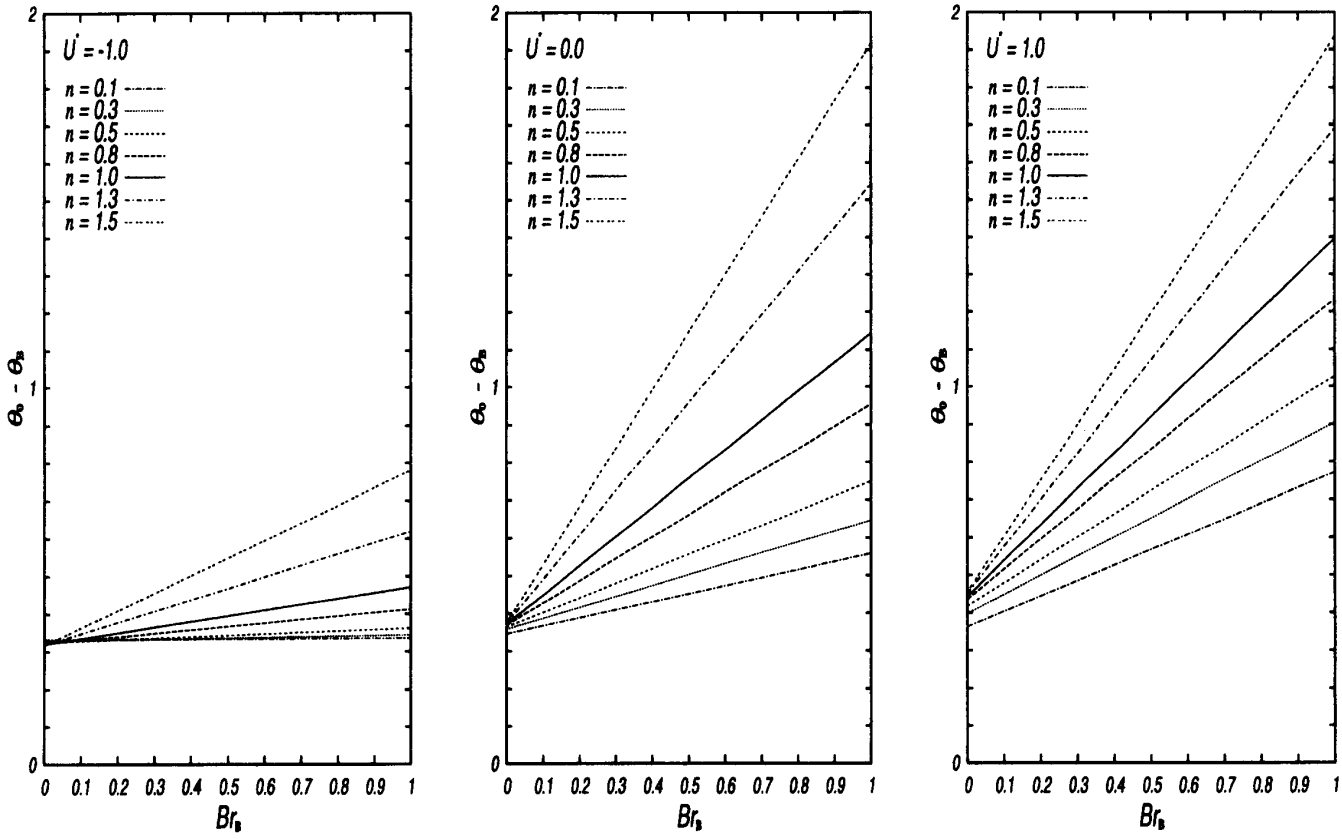

Fig. 5 Dimensionless temperature difference $(\theta_0 - \theta_B)$ for Case B

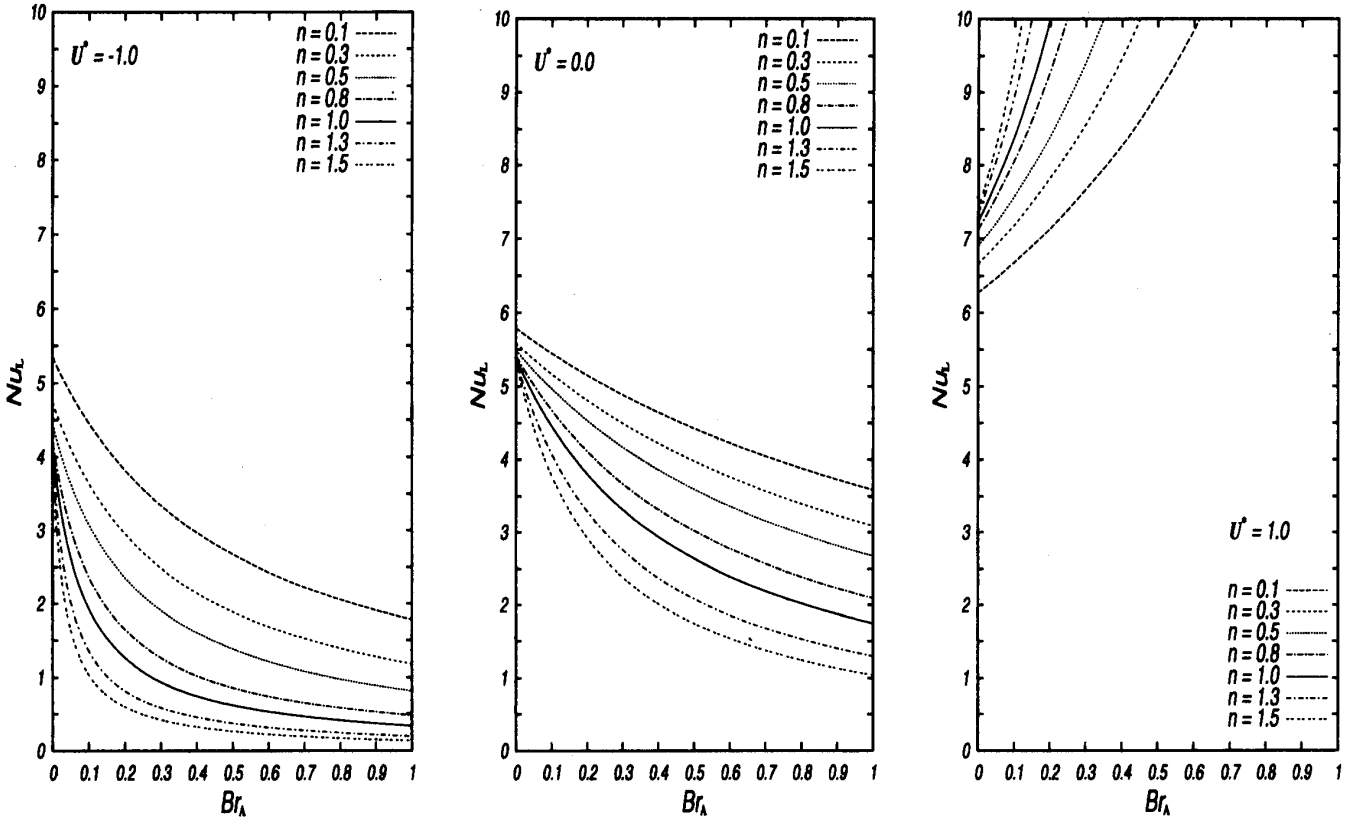

Fig. 6 Nusselt numbers for Case A

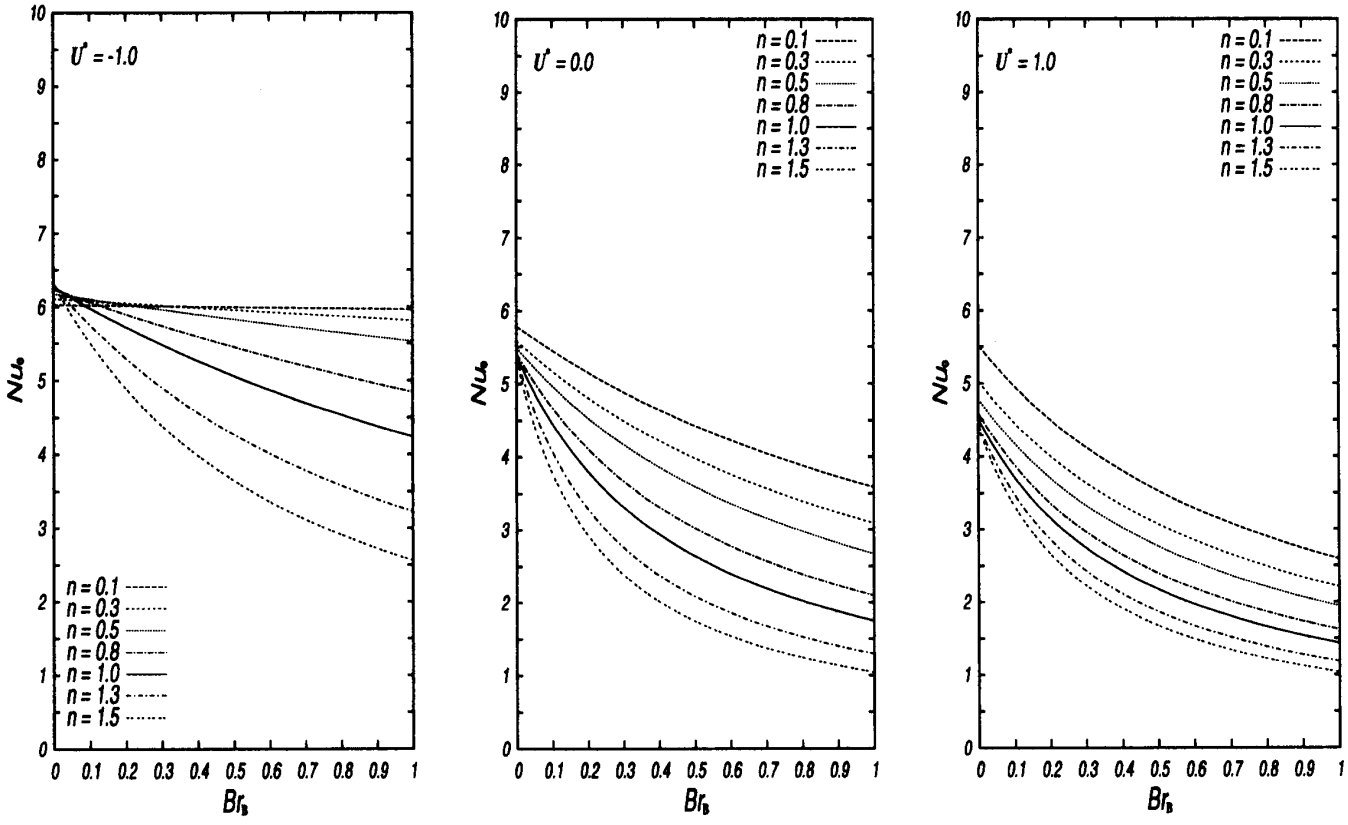

Fig. 7 Nusselt numbers for Case B

Appendix : Nuselt number, Nu_L and Nu_0

Case A with CASE Ⅰ Velocity Profile :

$$\theta_L-\theta_B=\int_0^1 u^*(\theta_L-\theta)dy^*=-\left[\int_0^{L^*_{max}} u_a^*(\theta_a-\theta_L)dy^*+\int_{L^*_{max}}^1 u_b^*(\theta_b-\theta_L)dy^*\right] \tag{A-1}$$

Integrating Eq.(A-1), we have

$$\theta_L-\theta_B=-\left(\frac{n}{n+1}\right)F^{\frac{1}{n}}[S_{A1}+S_{A2}] \tag{A-2}$$

where S_{A1} and S_{A2} are

$$S_{A1}=-\left(\frac{n+1}{2n+1}\right)(1-L^*_{max})L^{*\frac{2n+1}{n}}_{max}-\frac{1}{2}(1-L^*_{max})^2L^{*\frac{n+1}{n}}_{max}$$
$$+\frac{n^2}{(2n+1)(3n+1)}(1-L^*_{max})^{\frac{3n+1}{n}}+F^{\frac{1}{n}}D_{A1} \tag{A-3}$$

$$S_{A2}=Br_AF^{\frac{n+1}{n}}[\{1-U^*(1-L^*_{max})\}D_{A1}+D_{A2}] \tag{A-4}$$

D_{A1} and D_{A2} are

$$D_{A1}=\left(\frac{n}{n+1}\right)\left[-\frac{(n+1)^2(9n+2)}{3(3n+1)(4n+1)(5n+2)}L^{*\frac{5n+2}{n}}_{max}+\left(\frac{n+1}{4n+2}\right)(1-L^*_{max})^2L^{*\frac{3n+2}{n}}_{max}\right.$$
$$+\frac{1}{6}(1-L^*_{max})^3L^{*\frac{2n+2}{n}}_{max}-\frac{n(n+1)}{(2n+1)(3n+1)}(1-L^*_{max})^{\frac{3n+1}{n}}L^{*\frac{2n+1}{n}}_{max}$$
$$-\frac{n(8n^2+5n+1)}{2(2n+1)(3n+1)(4n+1)}(1-L^*_{max})^{\frac{4n+1}{n}}L^{*\frac{n+1}{n}}_{max}$$
$$\left.+\frac{n^3}{(2n+1)(3n+1)(5n+2)}(1-L^*_{max})^{\frac{5n+2}{n}}\right] \tag{A-5}$$

$$D_{A2}=\left(\frac{n}{2n+1}\right)\left[\frac{(n+1)(2n+1)(9n+2)}{2(3n+1)(4n+1)(5n+2)}L^{*\frac{5n+2}{n}}_{max}-\left(\frac{n+1}{3n+1}\right)(1-L^*_{max})^{\frac{3n+1}{n}}L^{*\frac{2n+1}{n}}_{max}\right.$$
$$\left.-\frac{1}{2}\left(\frac{2n+1}{4n+1}\right)(1-L^*_{max})^{\frac{4n+1}{n}}L^{*\frac{n+1}{n}}_{max}+\frac{n^2}{(3n+1)(5n+2)}(1-L^*_{max})^{\frac{5n+2}{n}}\right] \tag{A-6}$$

The Nusselt number on the moving plate, Nu_L, is obtained as

$$Nu_L=\frac{2}{-\left(\frac{n}{n+1}\right)F^{\frac{1}{n}}[S_{A1}+S_{A2}]} \tag{A-7}$$

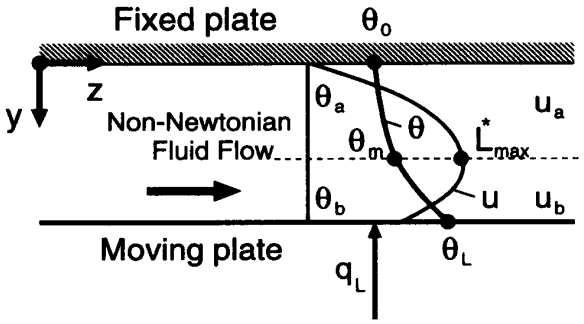

Fig.A-1 Temperature profile assumed in this analysis (Case A with Case Ⅰ)

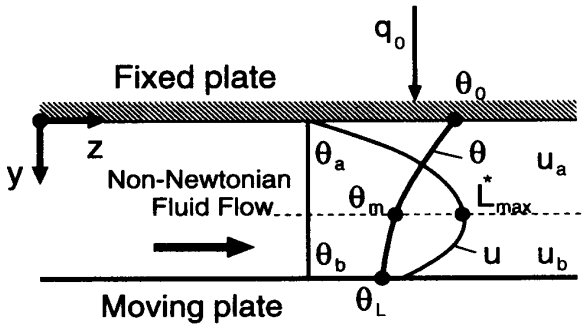

Fig.A-2 Temperature profile assumed in this analysis (Case B with Case Ⅰ)

Case B with CASE Ⅰ Velocity Profile

$$\theta_0-\theta_B=\int_0^1 u^*(\theta_0-\theta)dy^*=-\left[\int_0^{L^*_{max}} u_a^*(\theta_a-\theta_0)dy^*+\int_{L^*_{max}}^1 u_b^*(\theta_b-\theta_0)dy^*\right] \tag{A-8}$$

Integrating Eq.(A-8), we have

$$\theta_0-\theta_B=-\left(\frac{n}{n+1}\right)F^{\frac{1}{n}}[S_{B1}+S_{B2}] \tag{A-9}$$

where S_{B1} and S_{B2} are

$$S_{B1}=-\frac{(n+1)(4n+1)}{2(2n+1)(3n+1)}L_{max}^{*\frac{3n+1}{n}}-(1-L^*_{max})L_{max}^{*\frac{2n+1}{n}}+\left(\frac{n}{2n+1}\right)(1-L^*_{max})^{\frac{2n+1}{n}}L^*_{max}+F^{\frac{1}{n}}D_{B1} \tag{A-10}$$

$$S_{B2}=Br_BF^{\frac{n+1}{n}}[\{1-U^*(1-L^*_{max})\}D_{B1}+D_{B2}] \tag{A-11}$$

D_{B1} and D_{B1} are

$$\begin{aligned}D_{B1}=&\left(\frac{n}{n+1}\right)\left[-\frac{n(32n^3+39n^2+15n+2)}{2(2n+1)(3n+1)(4n+1)(5n+2)}L_{max}^{*\frac{5n+2}{n}}+\frac{1}{2}L_{max}^{*\frac{4n+2}{n}}-\frac{1}{3}L_{max}^{*\frac{2n+2}{n}}\right.\\&-\left(\frac{n}{3n+1}\right)(1-L^*_{max})L_{max}^{*\frac{4n+2}{n}}+(1-L^*_{max})L_{max}^{*\frac{3n+2}{n}}-\left(\frac{n}{3n+1}\right)(1-L^*_{max})^{\frac{2n+1}{n}}L_{max}^{*\frac{3n+1}{n}}\\&+\frac{1}{2}\left(\frac{n}{2n+1}\right)(1-L^*_{max})^{\frac{2n+1}{n}}L_{max}^{*\frac{n+1}{n}}-\left(\frac{n}{2n+1}\right)(1-L^*_{max})^{\frac{3n+1}{n}}L_{max}^{*\frac{2n+1}{n}}\\&\left.+\frac{n(8n^2+7n+1)}{2(2n+1)(3n+1)(4n+1)}(1-L^*_{max})^{\frac{4n+1}{n}}L_{max}^{*\frac{n+1}{n}}-\frac{2n^2}{(3n+1)(5n+2)}(1-L^*_{max})^{\frac{5n+2}{n}}\right]\end{aligned} \tag{A-12}$$

$$\begin{aligned}D_{B2}=&\left(\frac{n}{2n+1}\right)\left[-\frac{22n^3+35n^2+15n+2}{2(3n+1)(4n+1)(5n+2)}L_{max}^{*\frac{5n+2}{n}}-\left(\frac{2n+1}{3n+1}\right)(1-L^*_{max})L_{max}^{*\frac{4n+2}{n}}\right.\\&-\frac{1}{2}\left(\frac{n+1}{3n+1}\right)(1-L^*_{max})^{\frac{2n+1}{n}}L_{max}^{*\frac{3n+1}{n}}+\frac{1}{2}(1-L^*_{max})^{\frac{2n+1}{n}}L_{max}^{*\frac{n+1}{n}}-(1-L^*_{max})^{\frac{3n+1}{n}}L_{max}^{*\frac{2n+1}{n}}\\&\left.-\frac{n^2}{(3n+1)(4n+1)}(1-L^*_{max})^{\frac{4n+1}{n}}L_{max}^{*\frac{n+1}{n}}-\frac{2n(2n+1)}{(3n+1)(5n+2)}(1-L^*_{max})^{\frac{5n+2}{n}}\right]\end{aligned} \tag{A-13}$$

The Nusselt number on the fixed plate, Nu_0, is obtained as

$$Nu_0=\frac{2}{-\left(\frac{n}{n+1}\right)F^{\frac{1}{n}}[S_{B1}+S_{B2}]} \tag{A-14}$$